CARBON 97 (2016) 126–133

Contents lists available at ScienceDirect

CARBON

journal homepage: www.elsevier.com/locate/carbon

Gadolinium-functionalised multi-walled carbon nanotubes as a T_1 contrast agent for MRI cell labelling and tracking

Ania Servant [a], Igor Jacobs [b], Cyrill Bussy [a], Chiara Fabbro [c], Tatiana da Ros [c], Elzbieta Pach [d], Belen Ballesteros [d], Maurizio Prato [c], Klaas Nicolay [b], Kostas Kostarelos [a,*]

[a] Nanomedicine Lab, Faculty of Medical & Human Sciences & National Graphene Institute, University of Manchester, AV Hill Building, Manchester M13 9PT, UK
[b] Biomedical NMR, Department of Biomedical Engineering, Eindhoven University of Technology, Eindhoven, The Netherlands
[c] Center of Excellence for Nanostructured Materials, Department of Pharmaceutical Sciences, University of Trieste, Trieste, Italy
[d] Institut Català de Nanociència i Nanotecnologia (ICN2), Campus UAB, 08193 Bellaterra (Barcelona), Spain

ARTICLE INFO

Article history:
Received 19 June 2015
Received in revised form 14 August 2015
Accepted 17 August 2015
Available online 28 August 2015

Keywords:
MWNTs
Gadolinium
HUVEC
Cell labelling
T_1-weighted MRI
Endosomal entrapment

ABSTRACT

The development of efficient contrast agents for cell labelling coupled with powerful medical imaging techniques is of great interest for monitoring cell trafficking with potential clinical applications such as organ repair and regenerative medicine. In this paper, functionalised multi-walled carbon nanotubes (MWNTs) were engineered for cell labelling in T_1-weighted MRI applications. These sophisticated constructs were covalently functionalised with the gadolinium (Gd) chelating agent, diethylene triamine pentaacetic acid (DTPA), enabling tight attachment of Gd atoms onto the nanotube surface. The resulting Gd-labelled MWNTs were found to be stable over 2 weeks in water and mouse serum and high payload of Gd atoms could be loaded onto the nanotubes. The r_1 relaxivity of the Gd-MWNTs was a 3-fold higher than of the clinically approved T_1 contrast agent Magnevist at a magnetic field strength of 7T. The contrast efficiency, expressed as the r_1 relaxivity, of the Gd-MWNTs in Human Umbilical Vein Endothelial cells (HUVEC) was investigated at 7T and was found to be around 6.6 $mM^{-1}\,s^{-1}$. There was no reduction of the contrast efficiency after internalisation in HUVECs, which was imparted to the ability of carbon nanotubes to translocate the cell membrane.

1. Introduction

The ability to combine molecular and cellular imaging using a single medical imaging technique has attracted significant attention over the past few decades [1–5]. Examples of such imaging platforms include Positron Emission Tomography (PET), Magnetic Resonance Imaging (MRI), X-ray Computed Tomography (CT), and Single Photon Emission Computed Tomography (SPECT). All these techniques are non-invasive and enable real time visualization of cellular functions of living organisms and related molecular interactions [6–10]. MRI allows the visualisation of deep tissue, including soft tissues at high spatial and temporal resolution without the use of external ionising radiation or internal radiotracers, which makes it a preferable technique for imaging sensitive organs. While molecular MRI achieves specific imaging of molecular structures, specifically proteins that could be involved in specific diseases, cellular MRI imaging enables the visualisation of the whole cell with no discrimination between sub-cell structures or molecules [11–14].

Nevertheless, the resolution and imaging sensitivity of MRI relies heavily on the use and performance of metallic contrast agents. In the case of T_1-weighted MRI images, gadolinium (Gd) based compounds, including chelated complex molecules such as gadopentetate dimeglumine (Magnevist®) have been utilised as contrast agents pre-clinically for *in vitro* cell labelling to enable *in vivo* tracking and monitoring of stroke lesions or tumour growth [15–16]. The success and challenge of this technology is closely correlated to the ability of generating maximum effect on the relaxation rate of water protons. Although such Gd-based compounds are clinically approved and are widely employed in the clinical setting, some concerns have been raised due to the possible toxic side effects from the instability of these complexes in acidic environments and the release of free Gd^{3+} [17–18]. Research efforts have intensified on the development of sophisticated vectors that could encapsulate high payloads of gadolinium, including liposomes, dendrimers, micelles, carbon nanotubes (CNTs) and

* Corresponding author at: Nanomedicine Lab, Faculty of Medical & Human Sciences & National Graphene Institute, University of Manchester, AV Hill Building, Manchester M13 9PT, UK.
E-mail address: kostas.kostarelos@manchester.ac.uk (K. Kostarelos).

http://dx.doi.org/10.1016/j.carbon.2015.08.051
0008-6223/

micro-emulsions in addition to gadolinium chelates with high molar relaxivities [19–20].

Despite recent progress made in using CNTs for diagnostics and medical imaging, their use in this field remains an important challenge. For MRI applications, the coupling of CNTs with iron oxide superparamagnetic nanoparticles have been explored for developing contrast agents with effect on T_2 and T_2^* relaxation times [16,21–23]. Several strategies have also been examined for the development of gadolinium (Gd)-functionalised CNTs as contrast agents for T_1-weighted images [15]. Gadonanotubes [24–25] based on the nanoscale confinement of significant quantities of gadolinium atoms physically grafted (either onto sidewall defects or at the open ends) within the carbon backbone of ultra-short single-walled CNTs, were first reported as T_1-MRI contrast agents, followed by CNT-Gd oxide complexes and physical adsorption of Gd^{3+} chelates onto CNT surfaces [26]. Although these Gd-CNT complexes demonstrated very high r_1 relaxativity (relaxation rate enhancement per millimolar concentration of agents), most of these entities have not been investigated in an *in vivo* set-up due to their poor dispersibility in aqueous media. More recently, oxidised multi-walled carbon nanotubes covalently functionalised with the Gd^{3+} chelating agent diethylene triamine pentaacetic acid (DTPA) were investigated as a means to visualise and monitor the fate of CNTs *in vivo* after intravenous injection in small animals [27]. These Gd-functionalised CNTs were found to display a positive contrast in T_1-weighted images with a relatively high r_1 relaxivity suitable for tracking CNTs *in vivo*.

The ability of chemically functionalised carbon nanotubes to translocate the cell membrane has been described by various reports and different groups, and is now viewed as an efficient way to obtain direct access to the cell cytoplasm making them ideal for cargo delivery into cells [28]. In the case of MRI technology, such translocation effect might be of critical importance for cellular tagging for cell trafficking applications. Indeed the ability of monitoring transplanted cells *in vivo* and their tissue distribution offers critical understanding of cell migration in the body. The visualisation of successfully implanted cells at the intended injection site is also very challenging and could be enabled using cell labelling and MRI technology. In the case of human stem cells such knowledge is crucial for translation into the clinic for regenerative medicine applications.

In recent work, targeted Gd-labelled liposomes were developed as a cell probe for T_1-weighted MR imaging [29]. In this study, Kok et al. demonstrated that the performance of the endocytosed gadolinium based liposomes strongly relied on their intracellular sub-localisation within HUVECs as well as their concentration and this could impair the *in vivo* effective relaxation enhancement of these contrast agents. Therefore, the design of Gd-based nanoparticles as contrast agents that do not undergo internalisation into cells by endocytosis pathways was suggested. For this reason, the use of Gd-CNT constructs as a cell probe for T_1-weighted imaging appears to be a good alternative.

In this study, we describe the development of Gd-functionalised CNTs as a cell probe for T_1-weighted cell tracking MRI applications. Gadolinium was conjugated to multi-walled carbon nanotubes (MWNTs) via covalent functionalisation of the nanotube surface using the chelating molecule DTPA. Gd^{3+} cations are known to form very strong complexes with DTPA with a high association constant leading to very stable Gd-MWNTs conjugates. The Gd-MWNT conjugates were characterised using different techniques. The effective relaxation enhancement was characterised and measured using T_1- and T_2-measurements of Gd-MWNT conjugates in water and the gadolinium content was corroborated with elemental analysis. The *in vitro* magnetic resonance relaxivity of the constructs was investigated in human umbilical vein derived endothelial cells (HUVECs) as a model cell. Cell viability assays were also performed in order to assess the possible cytotoxic effects of the Gd-MWNT constructs.

2. Results and discussion

Multi-walled carbon nanotubes (MWNTs) were used as an engineering platform for designing novel MRI cell probes as they have demonstrated great ability to delivery drugs and other active substances to cells [30]. In addition, chemical functionalization of MWNTs in acidic conditions is known to further enhance their dispersibility in aqueous media by adding hydroxyl and carboxyl groups. In order to investigate the capability of MWNT as efficient cell probes, MWNTs were functionalised with DTPA. The chemical attachment of DTPA onto MWNT surfaces was performed by using a three step process as described in Fig. 1.

Following acid treatment, amine functionalities were added to MWNT 1 leading to the formation of MWNT 2 using 1,3-dipolar cycloaddition according to published procedures [31]. Amine groups are very useful for coupling molecules using a peptide-like bonding reaction with carboxylic acid groups [31]. MWNT 3 was obtained from MWNT 2 after coupling with DTPA. The functionalised carbon nanotubes MWNT 3 were fully characterised using standard analytic techniques and were found to display an approximate loading of 120 $\mu mol\ g^{-1}$ of DTPA.

The addition of Gd^{3+} to the carbon nanotube surface was performed by mixing MWNT 3 with Gd in a large excess in order to ensure a maximum of DTPA groups conjugated to Gd atoms. The labelling efficiency of Gd onto MWNT 3 sidewalls, defined as the ratio between the amount of Gd bound onto the carbon nanotube sidewall and the initial amount of Gd used for the complexation, was found to be optimal at 5 equivalents of Gd compared to the DTPA content (Fig. S1A). However, the maximum concentration of Gd chelated on MWNT 3 was achieved for 10 equivalents of Gd. Therefore, in order to maximise the contrast efficiency of the Gd-MWNT constructs, 10 equivalents of Gd were used for the con-

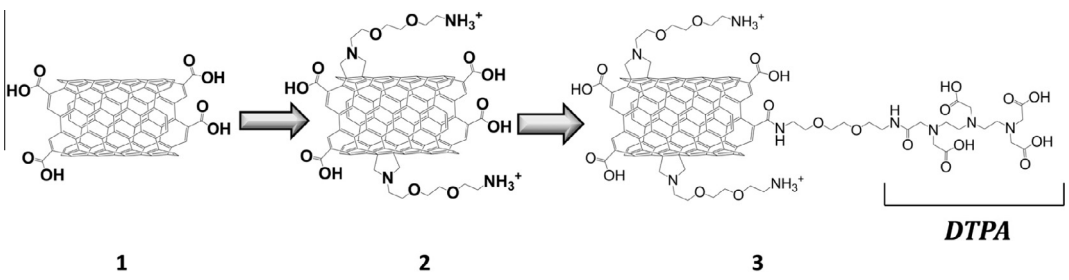

Fig. 1. Preparation of the carbon nanotube constructs for magnetic resonance (MR) and fluorescence imaging. Multi-walled carbon nanotube (MWNT) chemical functionalization from carboxylated MWNT (1). The latter were then modified into (2) introducing amino groups via 1,3 dipolar cycloaddition. DTPA ligand was introduced onto the amino MWNT by forming an amide bond using peptide chemistry resulting in (3).

jugation reaction. The Gd-MWNTs were then washed successively with water using ultracentrifugation. The presence of remaining free Gd atoms was characterised using xylenol orange. This spectrophotometric technique was developed using the property of xylenol orange to change colour when forming a complex molecule with free Gd atoms [32]. As a result, the amount of Gd atoms bound to the DTPA groups on the MWNT surface could be determined and was found to be around 33.5 μmol g^{-1} which corresponds to a yield of Gd conjugation of around 28%. In order to assess whether Gd is bound to MWNT 3 by conjugation to DTPA molecules or by adsorption onto the graphitic MWNT surface, a control experiment was performed by mixing MWNT 1 and MWNT 2 with an aqueous solution of Gd. No significant complexation of Gd^{3+} with bare MWNTs was observed implying that the Gd addition to the carbon nanotube surface was mainly occurring via conjugation with the chelating agent DTPA. The amount of Gd atoms conjugated to the DTPA groups of MWNT 3 was confirmed quantitatively by ICP-MS. The stability of the Gd-MWNT constructs prepared with different excesses of Gd in biological media was investigated (Fig. S1B i). The stability of the Gd-CNT construct with the highest Gd labelling efficiency was monitored over few days (6 days) by measuring the concentration of free Gd with ICP-MS and xylenol orange spectrophotometric technique (Fig. S1B ii). No significant amount of Gd was detected after 6 days; the release of Gd from the constructs was measured after 2 weeks in water and mouse serum and no detectable amount of Gd could be found in the release medium (data not shown).

In order to assess any structural damage of the sidewall of the MWNTs due to the chemical functionalization, electron microscopy analyses were conducted using high angle annular dark field high angle annular dark field (HAADF) scanning transmission electron microscopy (STEM) and SEM (Fig. 2A).

There was no significant damage on the nanotube sidewalls using SEM. Using HAADF-STEM, bright dots that were not present on the unlabelled MWNT 3 could be observed on the walls of labelled MWNTs indicating the presence of Gd atoms. HAADF-STEM is known to be a very effective technique enabling visualisation of heavy-element bearing molecules; intensity of HAADF-STEM images is directly correlated to the atomic number of the sample investigated [33–34]. The presence of Gd atoms on Gd-MWNTs was further confirmed by Energy Dispersive X-ray Spectroscopy EDX (Fig. S2).

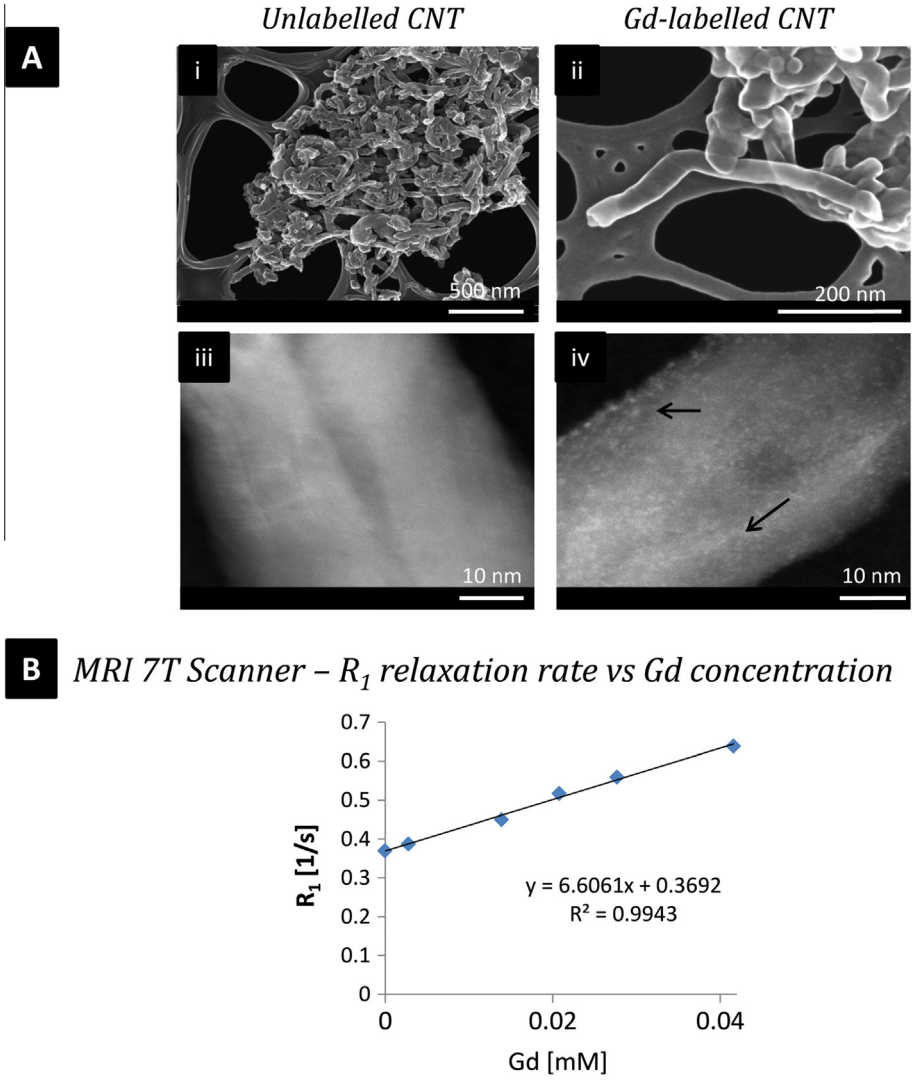

Fig. 2. Characterisation and contrast efficiency of gadolinium-labelled multi-walled carbon nanotubes (Gd-CNTs). (A) Physical characterisation of Gd-CNTs and unlabelled CNTs (**3**) with electron microscopy; scanning electron microscopy of carbon nanotube 3 (i) and of Gd-CNTs (ii) (Scale bars: 500 nm and 200 nm); high angle annular dark field (HAADF) scanning transmission electron microscopy (STEM) (iii) of carbon nanotube 3 and (iv) of Gd-CNTs; The presence of gadolinium on the labelled nanotubes could be evidenced by the bright spots on the nanotube backbone (black arrows). (Scale bars: 10 nm). (B) Determination of the contrast efficiency r_1 of Gd-CNTs that was found to be around 6.6 mM^{-1} s^{-1} (slope of the curve).

Gd-based MR contrast agents improve the contrast of MR images by reducing proton longitudinal relaxation times T_1 of protons in water molecules [35]. The contrast efficiency of the Gd-MWNT constructs produced was investigated using a 7T MRI instrument by measuring the longitudinal (T_1) and transversal relaxation (T_2) times in water at different Gd-MWNT concentrations (Fig. 2B for T_1, and Fig. S3 for T_2). The relaxivity that quantifies the contract efficacy of a contrast agent could be determined by using the relation $r_i = (R_i - R_{i,0})/[\mathrm{Gd}]$ ($i = 1,2$; $R_i = 1/T_i$, and $R_{i,0}$ is the endogenous relaxation rate). The relaxivity r_1 of the Gd-MWNT constructs was found to be 6.61 s^{-1} mM^{-1}. The transverse relaxivity r_2 of the Gd-MWNT constructs was also determined and was found to be 76.1 s^{-1} mM^{-1} (Fig. S3). Magnevist, Gd-DTPA, is a clinically approved MR contrast agents and is widely used in clinical procedures [36]. Magnevist displays a relaxivity r_1 of 2.1 s^{-1} mM^{-1} at 7T, making Gd-MWNTs (6.61 s^{-1} mM^{-1}) three times as efficient as the commercialised low molecular weight counterpart. The higher performance of the Gd-MWNTs compared to Magnevist's was explained by the local environment sensed by the paramagnetic centre. The high surface area of MWNTs enables Gd atoms to interact fully with the protons present in the medium. Similar results were obtained with other Gd-CNT constructs where a threefold relaxivity r_1 compared to that of Magnevist was demonstrated [27]. In addition, the Gd-MWNT constructs seemed to outperform the relaxivity r_1 of Gd-liposomes at similar magnetic field strengths [29]; the greater performance could be explained by the improved interaction of Gd atoms with protons in water as they are directly exposed to water molecules being located at the surface of the CNTs. In addition, local mobility of Gd atoms is known to have an effect on the relaxivity. In the case of Gd-MWNTs, Gd atoms are anchored to the nanotube surfaces reducing their local mobility; this is beneficial for the relaxivity as their tumbling rate is lower.

In order to assess the use of the Gd-MWNT constructs as efficient MRI cellular probes, cellular uptake was investigated on human umbilical vein derived endothelial cells (HUVECs) as a model of endocytotic cells. The contrast efficiency of Gd-based contrast agents depends greatly on the accessibility of water molecules to the Gd atoms; steric hindrance around Gd atoms that reduces its exposure to water protons is known to impair the relaxation effect of Gd. Therefore it is crucial to study the local environment of the Gd-MNWT constructs as well as their organisation in this environment, their intracellular location and the internalisation mechanism. HUVECs were selected as a model system as it has been previously reported that the longitudinal relaxivity r_1 of internalised targeted Gd-liposomes was much lower than non-targeted Gd-liposomes [29]. It was suggested that this relaxivity quenching effect for targeted Gd-liposomes was the result of the construct's confinement within endosomes, dramatically reducing Gd exposure to water protons from the bulk of the sample. This confinement within endosomes was imparted to the mechanism of internalisation that is different between targeted Gd-liposomes (internalisation via endocytosis) and non-targeted Gd-liposomes (non-endocytosis).

Here, HUVEC cells were exposed to different concentrations of Gd-MWNT constructs (0, 5, 10, 20, 35 or 40 μg ml^{-1}) and the cell viability was investigated at two time points (4 h and 24 h) (Fig. 3 and Fig. S4).

Unlabelled MWNT **3** were used as control. The internalisation of the carbon nanotubes was monitored over time by optical microscopy (phase contrast vs bright field) and internalisation of materials was clearly obvious after 24 h with cells turning partly black (Fig. 3 and S4A and B). Both types of carbon nanotubes (Gd-MWNT and MWNT 3) seemed to be localised within the cytoplasm of the HUVECs in a relatively diffused manner around the nucleus (see bright field images in Fig. 3A and Fig. S4B). The concentration of Gd internalised in cells after 4 h and 24 h at different Gd-MWNT concentration was also analysed by ICP-MS (Fig. 3B). The results demonstrated that internalisation of Gd-MWNT constructs increased from about 30% (of the initial Gd-MWNT exposing dose) at 4 h to about 50% at 24 h. Bright field images in Fig. 3A demonstrated that the amount of CNTs internalised per cell was dose dependent with a higher CNT content at 20 μg ml^{-1} as compared to 5 μg ml^{-1} for each type point considered. However, the internalisation of Gd-MWNT constructs in each cell pellets measured by ICP-MS was found to be similar for a considered time point and independent of the concentration of CNT used (~30% after 4 h of exposure and ~50% after 24 h for all three concentrations tested). After 4 and 24 h of exposure, there was no significant decrease of cell viability at increasing Gd-MWNT concentrations up to 40 μg ml^{-1} apart from the MWNT 3 at the highest concentration and after 24 h (Fig. 3C).

To assess the MRI properties of the Gd-labelled cells, HUVEC cell pellets were produced following incubation of cells with either Gd-MWNTs or MWNT 3 for 4 h or 24 h (Fig. 4A).

Subsequently, the relaxation rate of the cell pellets were measured and compared against the control cell pellets without any carbon nanomaterials (Fig. 4B). The relaxation rate R_1 of the HUVEC-internalised Gd-MWNTs demonstrated a significant contrast enhancement of approximately 1.5-fold compared to the HUVEC-internalised non-labelled MWNT cell pellets (Fig. 4B). While no difference between an incubation of 4 h and 24 h could be noticed for the non-labelled MWNTs (MWNT 3), an increase in R_1 could be observed between 4 h and 24 h for the cell pellets exposed to Gd-MWNT constructs. This was in agreement with the previous ICP-MS results showing an increase in internalisation percentage from 4 h to 24 h incubation from 30% to 50%. This led to an increase in Gd concentration in the cell pellets resulting in a greater increase in R_1. In order to evaluate the efficiency of the Gd-MWNT constructs as T_1-weighted cell probe for MRI, the relaxivity that is defined as the slope of the relaxation rate as a function of Gd concentration was determined (Fig. 4C). HUVECs were incubated with Gd-MWNTs and the non-labelled carbon nanotubes (MWNT 3) at increasing CNT concentrations (0, 10, 20, 25, 35, 40 μg/ml) for 24 h in order to have a wide range of Gd concentration inside the cells. The concentration of gadolinium inside the cell pellets was determined by ICP-MS and was found to range from 0.002 to 0.04 mM (data not shown). The relaxation rate R_1 of the cell pellets were then measured and plotted against Gd concentration in order to determine the relaxivity r_1 that was found to be 6.6 s^{-1} mM^{-1} (Fig. 4C). This value of r_1 was very similar to that of Gd-MWNT constructs alone ($r_1 = 6.61$ s^{-1} mM^{-1}) and was almost sixfold higher than the r_1 obtained with targeted Gd-liposomes, when extrapolating the values from the r_1 curve [29]. This indicated that there was no r_1-reducing effect following internalisation of the constructs in HUVECs. This represents a significant advantage of Gd-labelled MWNTs over other Gd-based nanoparticles such as liposomes where a dramatic quenching was observed, that was attributed to subcellular compartmentalization of the latter nanomaterials [29].

Several studies have reported the ability of carbon nanotubes to enter cells via passive diffusion through membranes, known as the 'needle effect', suggesting a different mechanism of internalisation from conventional endocytic pathways [28]. Marangon et al. demonstrated the use of Gd-labelled carbon nanotubes as efficient T_1-weighted MRI contrast agents in an *in vivo* set-up [27]. In this study, it was shown that, although most carbon nanotubes were gathered in large bundles within vesicular membranes when internalised in mouse macrophages, a small fraction of isolated tubes could be identified in the cytoplasm implying a small proportion of carbon nanotubes internalised by the 'needle effect'. In our study, HUVECs were used as a model of cells using endocytosis

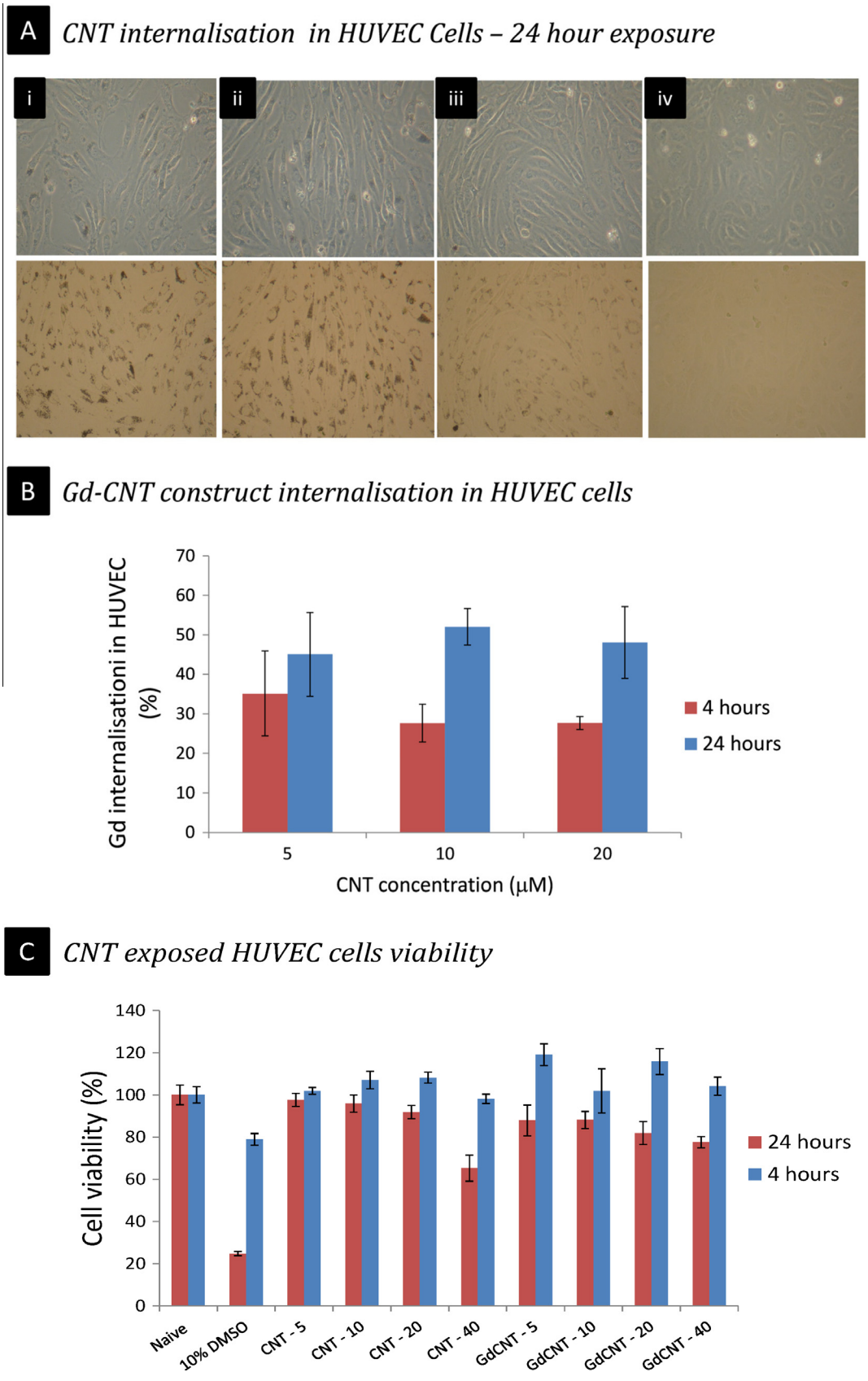

Fig. 3. Gd-CNT cell interactions, internalisation and cell viability. (A) Images of HUVEC cells exposed with (i) 20 μg/ml, (ii) 10 μg/ml, (iii) 5 μg/ml, and (iv) 0 μg/ml of Gd-CNTs for 24 h, scale bar = 100 μm; phase contrast imaging (higher panel) is compared to bright field imaging (lower panel) in which cells not exposed to CNTs have no contrast; (B) Gd-CNT cell internalisation over time assessed via ICP-MS; Cells were exposed to Gd-CNTs at different concentrations (5, 10, 20 μg/ml) for 4 and 24 h and the concentration of gadolinium inside cell pellets was measured by ICP-MS; (C) Cell viability of HUVEC cells exposed for 4 and 24 h with non-labelled CNTs and Gd- CNTs (0–40 μg/ml) assessed with a modified LDH assay.

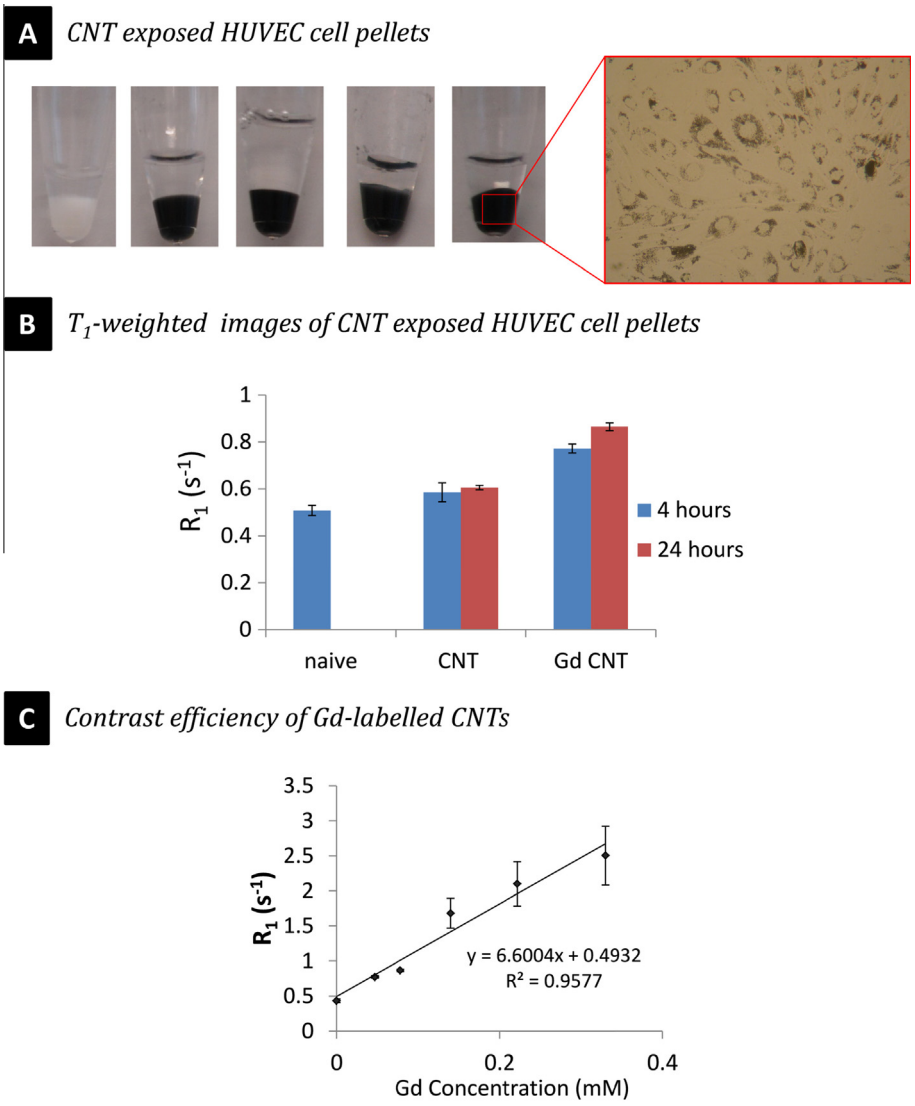

Fig. 4. Contrast efficiency of Gd-CNT for cell labelling using MRI. (A) CNT exposed HUVEC cell pellets. HUVEC cells were exposed to Gd-CNTs and non labelled CNTs for (first two black tubes) 24 h (second two black tubes) at different Gd-CNT concentrations, a control sample of unexposed HUVEC cell pellet (white tube) was also prepared. Prior to the formation of the pellets, the internalisation of Gd-CNTs was monitored using optical microscopy; (B) MRI characterisation of Gd-CNT internalised HUVEC cells; R_1 values of treated and untreated HUVEC (20 μg l^{-1} of Gd-MWNT construct) cells exposed for 4 and 24 h. (C) Contrast efficiency of Gd-CNTs as new cell probe; R_1 values versus gadolinium concentration (a. 0 μM, b. 4.2 μM; c. 8.1 μM; d. 13.9 μM; e. 20.8 μM; f. 35.5 μM).

pathways to internalise molecules and nanoparticles. These cells were shown to quench the contrast efficiency of targeted Gd-labelled liposomes after internalisation by endocytosis pathway [29]. This was explained by the compact confinement of the Gd-labelled liposomes in intracellular vesicles limiting the exchange between bulk water protons (which is needed for achieving a strong T_1 relaxation rate enhancement) and gadolinium atoms. The size and inherently the surface area of these vesicles were found to be a crucial parameter in the water proton and gadolinium interaction as larger vesicles display smaller surface-to-ratio limiting an efficient exchange between water protons and gadolinium atoms.

In our study, no quenching was observed after internalisation of the Gd-labelled MWNT in cells; the same relaxivity value was indeed obtained in both cell pellets and water (Fig. 4C and Fig. 2B respectively). This suggested that either a large quantity of carbon nanotubes did not internalise following endocytosis pathways or the vesicles in which they are located are small enough to enable efficient exchange between water protons and gadolinium atoms. Several studies in our group have confirmed the tendency of CNTs to internalise by piercing the cell membrane and subsequently avoiding endosome entrapment [37]. The absence of endosomal entrapment could explain why no quenching of T_1 relaxivity effects was observed with Gd-MWNTs.

3. Conclusion

This study demonstrated the great potential of using functionalised multi-walled carbon nanotubes (MWNTs) as efficient cell probes for MRI. At the same magnetic field strength, Gd-labelled MWNTs demonstrated great contrast enhancement in water in terms of a 3-fold increase in longitudinal relaxivity compared to Magnevist, the commercially and widely used in clinical procedures MR contrast agent. These sophisticated constructs also demonstrated great contrast enhancement with a high relaxivity value of 6.6 s^{-1} mM^{-1} after internalisation in HUVECs similar to that of the material dispersed in water. Quenching of MRI contrast agent efficacy *in vitro* and *in vivo* is of a great concern as it will hamper the detection of these agents with MRI. Efficient cell

probes and cell labelling are crucial for medical imaging in particular MRI applications as it could bring a better understanding of cell interaction and distribution in the human body and potentially limit the toxicity and side effects involved with Gd-based contrast agents. These functionalised MWNTs, thanks to their large surface area allowing higher payload of gadolinium pave the way to a new generation of Gd-based contrast agents enabling strong contrast enhancement and potentially reduced toxicity.

4. Experimental

4.1. Chemical functionalisation of MWNTs

Starting multi-walled carbon nanotubes (MWNTs) were purchased from Nanostructured and Amorphous Materials Inc. (Houston, USA) (stock #1240XH: 94% purity, outer diameter 20–30 nm, length 0.5–2 μm). Starting materials were first oxidised by acid treatment to generate MWNT 1, then MWNT 2 was obtained by using 1,3-dipolar cycloaddition reaction as previously reported [31]. After derivatization with DTPA, MWNT 3 was recovered by centrifugation, washed with water and re-precipitated from MeOH/diethyl ether. Kaiser tests confirmed a loading of 0.120 mmol g^{-1} of free amine after DTPA.

4.2. Gadolinium complexation

MWNT 3 were dispersed in water at a concentration of 0.5 mg/ml. Gadolinium chloride was added to the carbon nanotube solutions at increasing molar equivalents (1, 5, 10, 20, 50, 100, 500 eq.) compared to the evaluated DTPA quantity on the functionalised carbon nanotubes MWNT 3. The mixtures were allowed to incubate at room temperature for 1.5 h. The Gd-labelled carbon nanotubes were then washed three times with water and centrifuged in order to collect them. The quantity of Gd conjugated to MWNT 3 was determined by monitoring the free gadolinium during the washing steps using UV–Visible spectroscopy with the Xylenol Orange assay according to published procedures [32] and by elemental analysis using ICP-MS (Brucker).

4.3. Gd-labelled carbon nanotube characterisation

The Gd-labelled and unlabelled carbon nanotubes were characterised using HAADF-STEM images and EDX spectra were acquired on a FEI Tecnai G2 F20 HRTEM operated at 200 kV and equipped with an EDAX super ultra-thin window (SUTW) X-ray detector. Samples were deposited on lacey carbon Cu TEM grids (Agar) and using a high resolution transmission electron microscopy (HR-TEM), energy dispersive X-ray microscopy (EDX) using a JEOL ARM 200 F microscope operating at 80 kV.

4.4. MRI characterisation of Gd-labelled carbon nanotubes

All MRI measurements were performed on a 7 T Bruker BioSpec 70/30 USR (Bruker BioSpin MRI GmbH, Etlingen, Germany) equipped with a 1H 112/072 (outer/inner diameter) circular polarized MRI transceiver volume coil (Bruker BioSpin MRI GmbH, Etlingen, Germany) at room temperature. Eppendorf tubes containing the carbon nanotube samples in water were placed in a custom made holder filled with water to facilitate shimming. R_1 ($1/T_1$) measurements were performed with an inversion recovery segmented fast low angle shot (FLASH) sequence, with the following sequence parameters: T_R = 4 ms, T_E = 2 ms, FA = 8°, inversion time (TI) from 72.51 to 4792.51 ms in 60 steps, overall scan repetition time = 15 s, FOV = 40 × 40 mm^2, matrix size = 128 × 128, slice thickness = 1 mm and number of averages = 4.

R_2 ($1/T_2$) measurements were performed using a multi spin-echo sequence with the following sequence parameters: T_R = 2 s, T_E from 8 to 256 ms in 32 steps, FOV = 40 × 40 mm^2, matrix size = 128 × 128, slice thickness = 1 mm and number of averages = 4. The first echo was omitted from data analysis. Longitudinal and transverse relaxation rates were determined using Mathematica 8.0 (Wolfram Research Inc., Champaign, IL, USA) and plotted against the gadolinium concentration determined with ICP-MS. A linear least-squares fit was performed to determine the longitudinal and transverse relaxivities (mM^{-1} s^{-1}) of the MWNTs according to $r_{1,2} = \frac{R_{1,2}^{obs} - R_{1,2}^{dia}}{[Gd]}$, where $r_{1,2}$ is the longitudinal or transverse relaxivity (mM^{-1} s^{-1}), $R_{1,2}^{obs}$ (s^{-1}) is the measured longitudinal or transverse relaxation rate, $R_{1,2}^{dia}$ (s^{-1}) is the diamagnetic contribution and $[Gd]$ is the concentration of gadolinium (mM).

4.5. Cell culture

Human HUVECs were purchased from Lonza Bioscience, Basel, Switzerland (pooled donor, #C2519A). Cells were maintained on 1% gelatin-coated TCPS flasks with 10% FBS completed EGM-2 medium (Lonza Bioscience, Basel, Switzerland) and cultured in a humidified incubator at 37 °C with 5% CO_2. The EGM-2 medium was replaced every 2–3 days. Cells were sub-cultured when reaching 80–90% confluence according to supplier's instructions.

4.6. Preparation of cell pellets for MRI measurement and ICP-MS measurement

HUVECs of passage 3 or 4 were used for all experiments. To start the experiment, medium was replaced by either Gd-labelled or unlabelled carbon nanotubes containing medium at increasing carbon nanotube concentrations (0–40 μg/ml). After incubation for 4 or 24 h, the cells were washed twice with 5 mL of pre-warmed (37 °C) HEPES buffered saline solution (Lonza Bioscience, Basel, Switzerland). Cells in culture flasks were detached using 2 mL of 0.25% trypsin/1 mM EDTA solution (Lonza Bioscience, Basel, Switzerland). The trypsin/EDTA solution was neutralized using 4 mL of trypsin neutralizing solution (Lonza Bioscience, Basel, Switzerland). Cells were then spun down at 1400 rpm for 5 min; the supernatant was removed, the cell pellet was re-suspended in 1 ml of 4% PFA in PBS (Gibco, Life technologies) and finally transferred to a 500 μl Eppendorf tube until the MRI measurements.

For ICP-MS measurement, Gd-MWNT labelled HUVECs were prepared in a similar fashion. Once collected, cell pellets were re-suspended in pure nitric acid and boiled overnight to obtain a clear solution ideal for ICP-MS analysis.

4.7. Magnetic resonance imaging of cell pellets

Eppendorf tubes containing the cell pellets were placed in a custom made holder filled with water to facilitate shimming. Sagittal slices were planned through the length of the Eppendorf tubes. R_1 ($1/T_1$) and R_2 ($1/T_2$) were determined as described for the relaxivity measurements, with a FOV of 30 × 30 mm^2. Longitudinal and transverse relaxation rates were determined in a region of interested within the cell pellet using Mathematica 8.0 (Wolfram Research Inc., Champaign, IL, USA). The volume of the cell pellets was measured using a 3D FLASH sequence, with the following sequence parameters: T_R = 25 ms, T_E = 3.7 ms, FA = 30°, isotropic resolution = 0.1 mm, number of averages = 2. The pellet volume was determined by setting threshold values for the signal intensity to select the voxels within the cell pellet. The voxels within each pellet were multiplied by the voxel volume to determine the pellet volumes. The gadolinium content in each pellet determined by ICP-

MS was divided by the pellet volume to obtain the concentration of gadolinium within the pellet. Due to a lack of contrast, the volumes of the naïve cell pellets and the pellets incubated with unlabelled CNT could not be determined.

4.8. Cytotoxicity

HUVECs were seeded into 96-well plates (5000 cells/well) and cultured overnight before the experiment in a humidified incubator (5% CO_2, 37 °C). Culture medium was removed and replaced by culture medium containing Gd-labelled and unlabelled carbon at different carbon nanotube concentrations (0, 5, 10, 20, 40 μg/ml) nanotubes. HUVECs were incubated for 4 h and 24 h. After incubation with the carbon nanotubes, the cell viability was measured using the LDH assay as described in previous published reports [28].

Acknowledgements

A.S. would like to thanks the United Kingdom Engineering and Physical Sciences Research Council (EPSRC) (Grant No. EP/G061882/1) under the Grand Challenge in Nanotechnology: Healthcare scheme. C.B. acknowledges the financial support from the European Commission FP-7 Marie Skłodowska Curie Actions–Career Development Research Fellowship (NANONEUROHOP, PIEF-GA-2010-276051).

Appendix A. Supplementary data

Supplementary data associated with this article can be found, in the online version, at http://dx.doi.org/10.1016/j.carbon.2015.08.051.

References

[1] D.A. Benaron, Cancer Metastasis Rev. 21 (1) (2002) 45–78.
[2] H. Kobayashi et al., Chem. Rev. 110 (5) (2010) 2620–2640.
[3] N.K. Logothetis, Nature 453 (7197) (2008) 869–878.
[4] A.Y. Louie, Chem. Rev. 110 (5) (2010) 3146–3195.
[5] E. Terreno et al., Chem. Rev. 110 (5) (2010) 3019–3042.
[6] O. Rabin et al., Nat. Mater. 5 (2) (2006) 118–122.
[7] J.K. Willmann et al., Nat. Rev. Drug Discovery 7 (7) (2008) 591–607.
[8] Y.R. Huang et al., Nanoscale 4 (20) (2012) 6135–6149.
[9] M. de Smet et al., J. Control. Release 169 (1–2) (2013) 82–90.
[10] A.E. John et al., J. Nucl. Med. 54 (12) (2013) 2146–2152.
[11] A.A. Gilad et al., Nat. Biotechnol. 25 (2) (2007) 217–219.
[12] K.C. Briley-Saebo et al., J. Magn. Reson. Imaging 26 (3) (2007) 460–479.
[13] T. Cyrus et al., J. Cardiovasc. Magn. Reson. 9 (6) (2007) 827–843.
[14] W.J.M. Mulder et al., Top. Magn. Reson. Imag.: TMRI 18 (5) (2007) 409–417.
[15] C. Richard et al., Nano Lett. 8 (1) (2008) 232–236.
[16] B.T. Doan et al., Contrast Media Mol. Imaging 7 (2) (2012) 153–159.
[17] H.S. Thomsen, Eur. Radiol. 16 (12) (2006) 2619–2621.
[18] M. Edward et al., J. Pathol. 214 (5) (2008) 584–593.
[19] S. Langereis et al., NMR Biomed. 26 (7) (2013) 728–744.
[20] P. Caravan, Chem. Soc. Rev. 35 (6) (2006) 512–523.
[21] J.T.W. Wang et al., Adv. Funct. Mater. 24 (13) (2014) 1880–1894.
[22] G. Lamanna et al., Nanoscale 5 (10) (2013) 4412–4421.
[23] O. Vittorio et al., Nanotechnology 22 (9) (2011).
[24] K.B. Hartman et al., Nano Lett. 8 (2) (2008) 415–419.
[25] B. Sitharaman et al., Chem. Commun. 31 (2005) 3915–3917.
[26] B. Sitharaman et al., J. Appl. Phys. 113 (13) (2013).
[27] I. Marangon et al., Adv. Funct. Mater. 24 (45) (2014) 7173–7186.
[28] H. Ali-Boucetta et al., Small 7 (22) (2011) 3230–3238.
[29] M.B. Kok et al., Magn. Reson. Med. 61 (5) (2009) 1022–1032.
[30] C. Fabbro et al., Chem. Commun. 48 (33) (2012) 3911–3926.
[31] V. Georgakilas et al., Chem. Commun. 24 (2002) 3050–3051.
[32] A. Barge et al., Contrast Media Mol. Imaging 1 (5) (2006) 184–188.
[33] S.Y. Hong et al., J. Am. Chem. Soc. 129 (36) (2007) 10966–10967.
[34] P. Luksirikul et al., J. Mater. Chem. 21 (47) (2011) 19080–19085.
[35] G.J. Strijkers et al., Magn. Reson. Mater. Phys., Biol. Med. 18 (4) (2005) 186–192.
[36] B. den Adel et al., Atherosclerosis 225 (2) (2012) 274–280.
[37] K. Kostarelos et al., Nat. Nanotechnol. 2 (2) (2007) 108–113.